Materials Physics and Mechanics. 2022;50(1): 118-125
Research article
http://dx.doi.org/10.18149/MPM.5012022_9

Submitted: April 21, 2022
Approved: June 19, 2022
Accepted: August 17, 2022

Molecular dynamics simulation of severe plastic deformation of nanotwinned Hadfield steel

G.M. Poletaev[1]✉, R.Y. Rakitin[2]

[1]Altai State Technical University, Lenin Str. 46, 656038 Barnaul, Russia

[2]Altai State University, Lenin Str. 61, 656049 Barnaul, Russia

✉ gmpoletaev@mail.ru

Abstract. The features of the plastic deformation at the atomic level and the formation of a dislocation structure in nanotwinned Hadfield steel under severe shear deformation along the direction perpendicular to parallel coherent twins were studied by the method of molecular dynamics. Similar studies for comparison were carried out for austenite. Dislocations in steel propagated and developed more weakly than in austenite, stacking faults between partial dislocations were shorter, and the number of dislocations was smaller, which was a consequence of the interaction of dislocations with impurity carbon atoms in steel. The main plastic shifts inside the computational cells containing parallel twins occurred predominantly along twin boundaries in the form of twinning dislocations. Dislocations from another slip system, not parallel to the twin boundaries, practically did not form. As a result of the passage of twinning dislocations, the twins moved during deformation.
Keywords: molecular dynamics, deformation, nanotwinned metal, Hadfield steel

Acknowledgements*. No external funding was received for this study.*

Citation: Poletaev GM, Rakitin RY. Molecular dynamics simulation of severe plastic deformation of nanotwinned Hadfield steel. *Materials Physics and Mechanics*. 2022;50(1): 118-125. DOI: 10.18149/MPM.5012022_9.

1. Introduction

Hadfield steel, due to its excellent work hardening capacity [1,2], is of great practical importance and has a long history of research into its unique properties. At the same time, to date, there are very few works devoted to modelling its atomic structure and the processes occurring in it under deformation conditions at the atomic level, which is due, in particular, to the complexity of modelling such multicomponent systems. Currently, there are a number of questions related to the mechanisms of plastic deformation at the atomic level in steels and which can be solved mainly by computer simulation methods. Such issues include, for example, the features of the formation and propagation of dislocations depending on various factors, the mechanisms of interaction with each other, grain boundaries, twins, and other defects.

In recent years, it has been found that the introduction of a high density of coherent twin boundaries to grain domains can significantly improve the strength of materials [3,4]. Such phenomenon has been discovered in various materials such as copper, gold, high-entropy alloys, and steels [3-9]. For example, in [5] authors showed that the copper with nanometre-scale twins (in terms of both twin thickness and spacing) exhibits a tensile strength ten times

higher than that of the conventional coarse-grained copper. This excellent strengthening effect of nanotwins is attributed to their role as effective dislocation barriers, which reduce the dislocation mean free path and thereby promote dislocation multiplication, similar to the effect of grain boundaries [10]. In works [11-14], performed using computer simulation, it is shown that a coherent twin is a serious obstacle for a moving edge dislocation. Significant energy and stress are required to overcome a twin by an edge dislocation.

This work is devoted to studying, using molecular dynamics simulation, the features of plastic deformation at the atomic level and the formation of a dislocation structure in nanotwinned Hadfield steel under severe shear deformation along a direction perpendicular to parallel coherent twins. To determine and isolate the role of twins and impurity atoms in steel in the deformation process, studies were carried out in parallel on the example of four samples: Hadfield steel and fcc Fe without twins and containing parallel coherent twins.

2. Description of the model

Hadfield steel, as is known, is a multi-component system and, in addition to classical iron, manganese, and carbon, may contain some other alloying elements [1,2]. In this study, we limited to a system that included three elements: γ-Fe as a matrix, Mn, and C. To describe the Fe-Fe interactions in the austenite matrix, it was used Lau EAM potential [15], which reproduces well the structural, energy, and elastic characteristics of austenite [15,16]. For all other five interatomic interactions in the γ-Fe-Mn-C system, we used the Morse potentials found by us earlier in [17] based on experimental data on the dissolution energy and migration energy of the corresponding impurity atoms in the fcc iron crystal, the atomic radius, their electronegativity, mutual binding energy, and other characteristics.

The standard ratio of components was used: Mn – 13 wt.% and C – 1.2 wt.% (12.63 at.% and 5.33 at.%, respectively) [1,2]. Mn atoms were introduced into fcc iron lattice randomly by replacing Fe atoms. The binding energy of Mn and C atoms in austenite lattice is very high – 0.35 eV, according to [18], which is approximately the same as, for example, the binding energy of carbon atoms with vacancies (0.37–0.41 eV [19]). That is, Mn atoms are a kind of effective "traps" for impurity carbon atoms, not allowing them, in particular, to form clusters on dislocations and grain boundaries. In this connection, carbon atoms were introduced into the octahedral voids closest to Mn atoms. The number of carbon atoms has corresponded to a given concentration. The choice of Mn atoms near which C atoms were introduced, as well as the selection of one of the neighboring octahedral voids, were made randomly.

In pure fcc iron, which was considered in this work for comparison with Hadfield steel, the type of the crystal lattice remained constant over the entire temperature range; the polymorphic transformation was not taken into account in this work. As mentioned above, pure austenite was considered to determine the contribution of Mn and C impurities in the processes under study.

In this work, we considered the computational cells of fcc Fe and Hadfield steels, which initially did not contain defects (except for impurity atoms) (Fig. 1a) and contained four parallel coherent twins $\Sigma3(\bar{1}\bar{1}1)[\bar{1}10]$ (Fig. 1b). A total of four cells were considered. The computational cell of fcc Fe contained approximately 123 thousand atoms, while that of Hadfield steel contained 130 thousand atoms. It was 27.2 nm long, 20.3 nm high, and 2.5 nm thick. Thus, the distance between parallel twins was 6.8 nm, which does not contradict the data on the distance between twins in real materials [20]. Along the *X* and *Y* axes (Fig. 1), an infinite repetition of the structure was simulated, that is periodic boundary conditions were imposed. The shear in the model was initiated by the displacement of atoms in the upper and lower regions highlighted by light grey in Fig. 1 in opposite directions along and against the y-axis (the [111] direction). The areas in the upper and lower parts of the cell in the course of

the computer experiment moved as a whole. In our previous work [17], we selected the optimal shear rate for the molecular dynamics method in this case – 10 m/s.

The time integration step in the molecular dynamics method was 2 fs [21-23]. The simulation of the deformation was carried out at a temperature of 300 K. The temperature in the model was set through the initial velocities of the atoms according to the Maxwell-Boltzmann distribution. When setting the temperature, it was obligatory to take into account the thermal expansion of the crystal lattice. To do this, for the interatomic interaction potentials used in the work, the average thermal expansion coefficients were previously found in the molecular dynamics model: $18 \cdot 10^{-6}$ K^{-1} for γ-Fe and $16 \cdot 10^{-6}$ K^{-1} for Hadfield steel. To keep the temperature constant during the simulation, a Nose-Hoover thermostat was used.

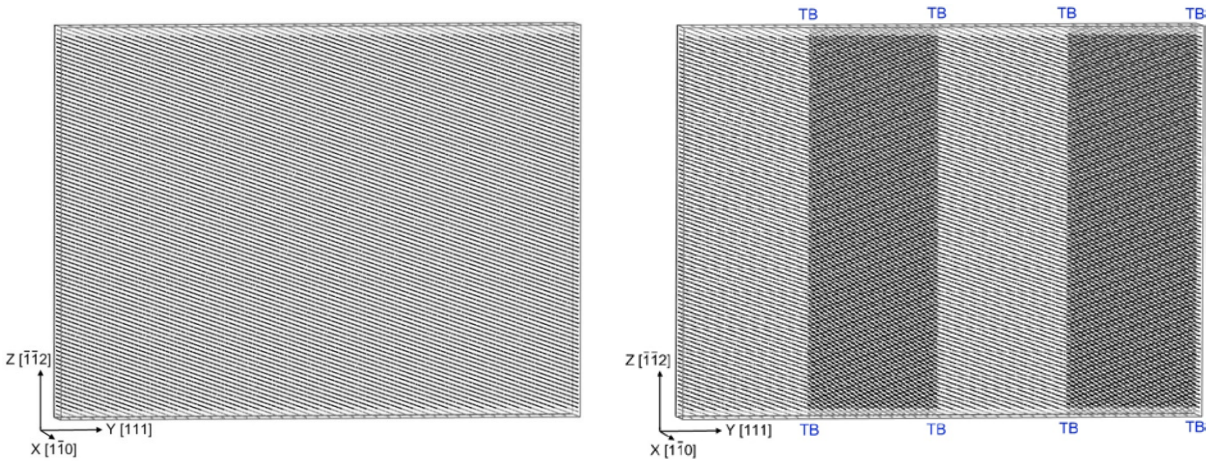

a) b)

Fig. 1. Computational cells for modelling the shear along the [111] direction (y-axis): a) without twins; b) containing four parallel twin boundaries (TB)

3. Results and discussion

To determine the mechanism of plastic deformation and the role of twins and impurity atoms in it, in this work, we studied the transformation of the structure during plastic shear in 15% and 30% of the considered computational cells. As is known, in crystals with an fcc lattice, the slip system {111}<110> is predominant [24,25]. During plastic shear along the <111> direction (y-axis), two slip systems are involved. The joint work of dislocations of two different slip systems is clearly seen, for example, in Fig. 2a, which shows the fcc Fe structure obtained after a 15% shear. In the figure, the computational cell is oriented in such a way that plastic shifts are better seen. Thin dark bands are mainly stacking faults separating partial dislocations. Relatively thick dark bands are the result of twinning. In Figure 2b, which shows the structure after a shear of 30%, this process is more pronounced. With such a large deformation, more complex defects are already formed: grain boundaries and parallel twins. There are fewer simple dislocations. In Figure 2b, near one of the cell borders (in this case, the upper one), along which the shear was performed, a low-angle grain boundary (GB in the figure) was formed, and the plastic shift proceeded mainly due to grain boundary sliding (GBS). Twins actively worked: the twin bands changed their width during deformation, which indicates the frequent passage of twinning dislocations along the twin boundary (TB) (in Fig. 2b one can clearly see such a twinning dislocation in the form of a step on TB in the centre of the computational cell). It is noteworthy that these twins ended at the grain boundary in the upper part of the cell.

The difference between pure austenite and steel, as can be seen in Fig. 3, is quite large and visible visually. Dislocations in steel propagated and developed much more weakly than in pure fcc iron, stacking faults between partial dislocations are noticeably shorter and their

number is smaller. Obviously, in this case, the work of impurity carbon atoms takes place, which, as is known, have positive binding energy both with dislocations and stacking faults [26-28], thereby slowing down the movement of dislocations.

In the case of steel, in contrast to pure austenite, the process of formation of parallel twins was not observed in the model. On the other hand, GBS manifested itself more clearly; it was the main mechanism of plastic deformation at a shear of 30% (Fig. 3b).

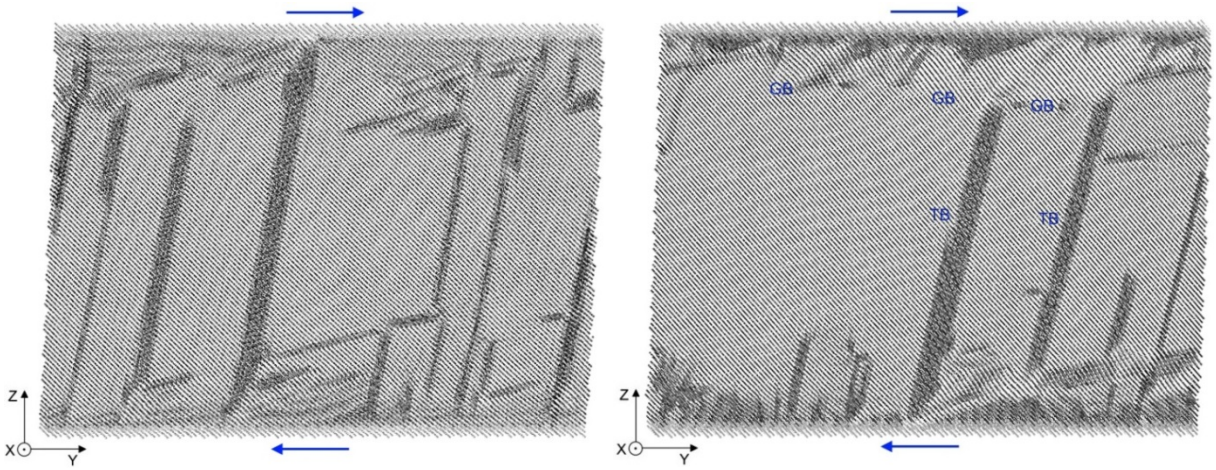

a) b)

Fig. 2. Structure of fcc Fe after a shear along the y-axis [111] by 15% (a) and 30% (b). GB – grain boundary, TB – twin boundary

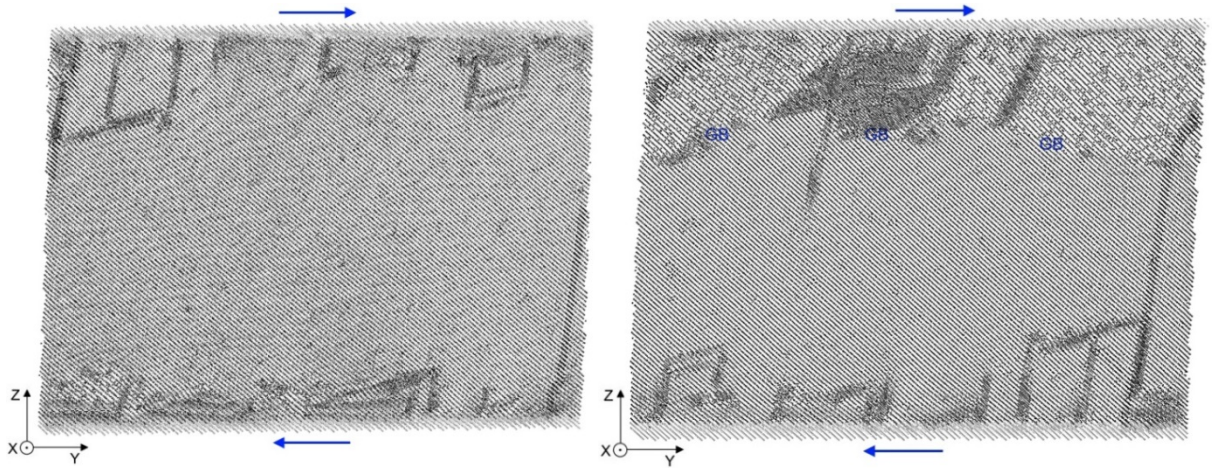

a) b)

Fig. 3. Structure of Hadfield steel after a shear along the y-axis [111] by 15% (a) and 30% (b)

Figure 4 shows the structures of the computational cell of fcc iron, initially containing four parallel twin boundaries at equal distances, deformed by shear along the [111] direction by 15% (Fig. 4a) and 30% (Fig. 4b). When considering the picture obtained with deformation of 15%, the first thing that attracts attention is the almost complete absence of dislocations from the slip system that is not parallel to the twin boundaries. And at the same time, there is a change in the distance between the twins. The displacement or migration of a twin boundary occurs, as is known, as a result of the passage of a twinning dislocation along the twin boundary [24,25]. The change in the distances between twins is the result of the passage of twinning dislocations. They could not go beyond the limits of the computational cell due to the rigid boundary conditions, as a result of which local deformations of the structure were formed in the computational cell near the upper and lower boundaries of the cell. In general,

there are noticeably fewer individual dislocations than in a pure crystal (Fig. 2a), because many of them in this case formed in the form of twinning dislocations, which are visible in the images as steps on twin boundaries. After passing along the twin boundary, they accumulated near the upper and lower boundaries of the computational cell. Intersections of twins by dislocations and shear through twins were not observed; as mentioned earlier, they represent a significant barrier to dislocations.

At a deformation of 30%, the mechanisms described above were supplemented by the formation of a low-angle grain boundary along the upper and lower boundaries of the computational cell and the occurrence of deformation also due to grain boundary sliding (Fig. 4b). It should be noted that the distance between the twins has changed even more, which indicates that the work of twinning dislocations continues.

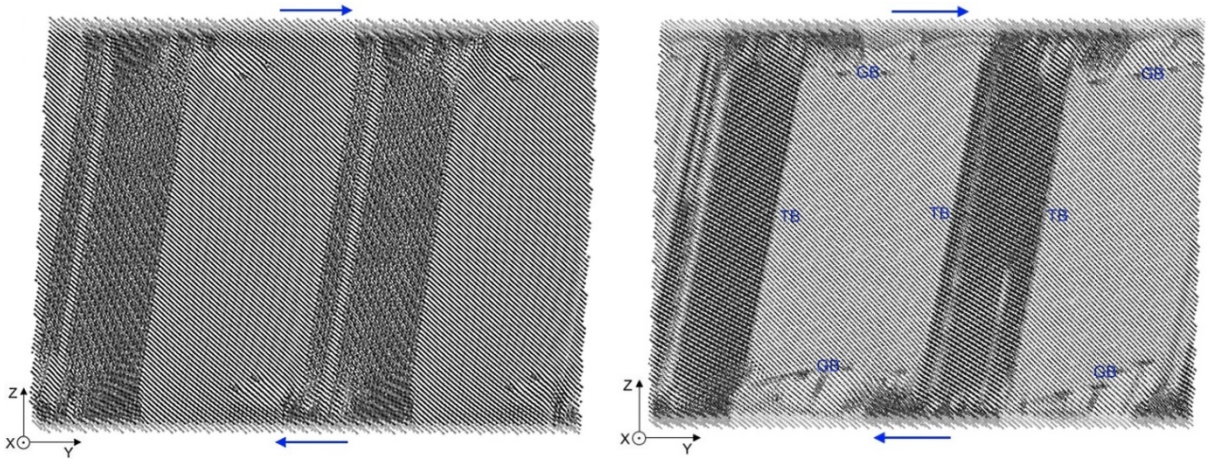

a) b)

Fig. 4. Structure of fcc Fe, which initially contained twins, after a shear along the y-axis [111] by 15% (a) and 30% (b)

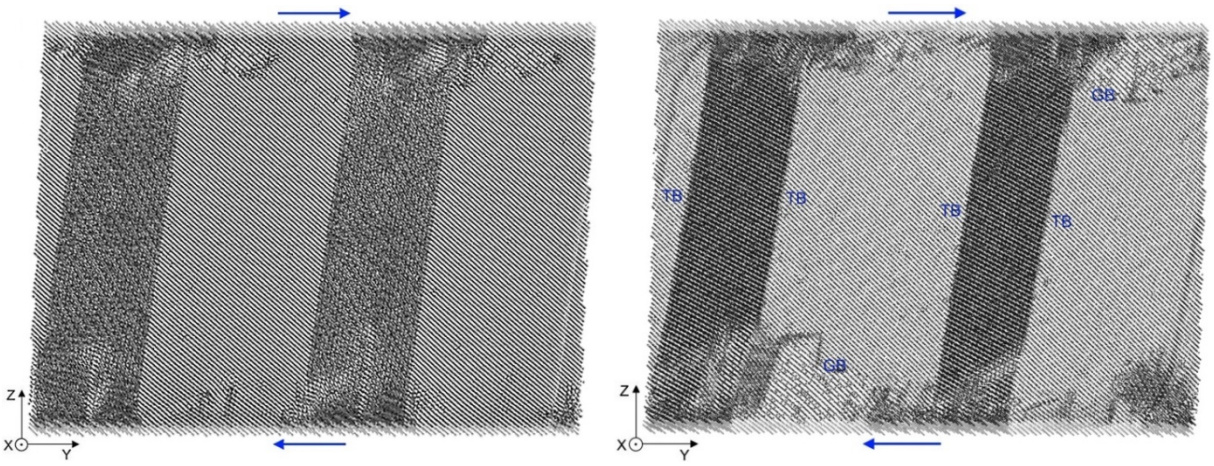

а) б)

Рис. 5. Structure of Hadfield steel, which initially contained twins, after a shear along the y-axis [111] by 15% (a) and 30% (b)

When performing a similar simulation of deformation in steel, all the mechanisms identified above for fcc iron also took place in Hadfield steel, with the difference that there were again much fewer individual dislocations than in iron. The main plastic shifts inside the computational cells occurred along the twin boundaries in the form of twinning dislocations – Fig. 5 shows how the distances between the twins changed as the deformation increased.

Crystalline grains between twins, except for the structure near the upper and lower borders of the cell, remained virtually defect-free.

4. Conclusion

The features of the plastic deformation at the atomic level and the formation of a dislocation structure in nanotwinned Hadfield steel under severe shear deformation along the direction perpendicular to parallel coherent twins were studied by the method of molecular dynamics. Similar studies for comparison were carried out for steel and fcc iron, not containing twins.

In pure fcc iron, which initially does not contain twins, plastic deformation in the considered type of deformation was carried out mainly due to the formation of dislocations in two slip systems. With an increase in deformation up to 30%, more complex defects (twins and grain boundaries) were formed; plastic deformation was carried out by twinning and grain boundary sliding.

Dislocations in steel propagated and developed much more weakly than in pure fcc iron, and stacking faults between partial dislocations were shorter. At a high strain of 30% in steel, in contrast to austenite, the process of formation of parallel twins was not observed in the model. On the other hand, grain boundary sliding manifested itself more clearly; it was the main mechanism of plastic deformation at a shear of 30%.

In the initial presence of twins, both in fcc iron and in steel, the main plastic shears inside the computational cells occurred predominantly along the twin boundaries in the form of twinning dislocations. Dislocations from another slip system, not parallel to the twin boundaries, practically did not form. As a result of the passage of twinning dislocations, the twins moved during deformation.

References

1. Zhang FC, Lv B, Wang TS, Zheng CL, Zhang M, Luo HH, Liu H, Xu AY. Explosion hardening of Hadfield steel crossing. *Materials Science and Technology*. 2010;26(2): 223-229.
2. Chen C, Lv B, Ma H, Sun D, Zhang F. Wear behavior and the corresponding work hardening characteristics of Hadfield steel. *Tribology International.* 2018;121: 389-399.
3. Lu K, Lu L, Suresh S. Strengthening materials by engineering coherent internal boundaries at the nanoscale. *Science*. 2009;324(5925): 349-352.
4. Sun L, He X, Lu J. Nanotwinned and hierarchical nanotwinned metals: a review of experimental, computational and theoretical efforts. *npj Computational Materials*. 2018;4: 6.
5. Lu L, Chen X, Huang X, Lu K. Revealing the maximum strength in nanotwinned copper. *Science*. 2009;323(5914): 607-610.
6. Zhou P, Liang ZY, Huang MX. Microstructural evolution of a nanotwinned steel under extremely high-strain-rate deformation. *Acta Materialia*. 2018;149: 407-415.
7. Li Q, Yan FK, Tao NR, Ponge D, Raabe D, Lu K. Deformation compatibility between nanotwinned and recrystallized grains enhances resistance to interface cracking in cyclic loaded stainless steel. *Acta Materialia*. 2019;165: 87-98.
8. Liu RD, Li YZ, Lin L, Huang CP, Cao ZH, Huang MX. Strain rate sensitivity of a 1.5 GPa nanotwinned steel. *Journal of Iron and Steel Research International.* 2021;28: 1352-1356.
9. Wang HT, Tao NR, Lu K. Strengthening an austenitic Fe-Mn steel using nanotwinned austenitic grains. *Acta Materialia*. 2012;60(9): 4027-4040.
10. Wang G, Li G, Zhao L, Lian J, Jiang Z, Jiang Q. The origin of the ultrahigh strength and good ductility in nanotwinned copper. *Materials Science and Engineering: A.* 2010;527(16-17): 4270-4274.

11. Jin Z-H, Gumbsch P, Albe K, Ma E, Lu K, Gleiter H, Hahn H. Interactions between non-screw lattice dislocations and coherent twin boundaries in face-centered cubic metals. *Acta Materialia.* 2008;56(5): 1126-1135.
12. Malyar NV, Grabowski B, Dehm G, Kirchlechner C. Dislocation slip transmission through a coherent Σ3{111} copper twin boundary: strain rate sensitivity, activation volume and strength distribution function. *Acta Materialia.* 2018;161: 412-419.
13. Liang Y, Yang X, Gong M, Liu G, Liu Q, Wang J. Interactions between dislocations and three-dimensional annealing twins in face centered cubic metals. *Computational Materials Science.* 2019;161: 371-378.
14. Chen C, Zhang F, Xu H, Yang Z, Poletaev GM. Molecular dynamics simulations of dislocation–coherent twin boundary interaction in face-centered cubic metals. *Journal of Materials Science.* 2022;57: 1833-1849.
15. Lau TT, Forst CJ, Lin X, Gale JD, Yip S, Van Vliet KJ. Many-body potential for point defect clusters in Fe-C alloys. *Physical Review Letters.* 2007;98(21): 215501.
16. Oila A, Bull SJ. Atomistic simulation of Fe-C austenite. *Computational Materials Science.* 2009;45(2): 235-239.
17. Poletaev GM, Rakitin RY. Molecular dynamics study of stress-strain curves for γ-Fe and Hadfield steel ideal crystals at shear along the <111> direction. *Materials Physics and Mechanics.* 2021;47(2): 237-244.
18. Massardier V, Le Patezour E, Soler M, Merlin J. Mn-C interaction in Fe-C-Mn steels: study by thermoelectric power and internal friction. *Metallurgical and Materials Transactions A.* 2005;36A: 1745-1755.
19. Slane JA, Wolverton C, Gibala R. Carbon-vacancy interactions in austenitic alloys. *Materials Science and Engineering A.* 2004;370(1-2): 67-72.
20. Zhu T, Gao H. Plastic deformation mechanism in nanotwinned metals: an insight from molecular dynamics and mechanistic modeling. *Scripta Materialia.* 2012;66(11): 843-848.
21. Poletaev GM, Zorya IV, Rakitin RY, Iliina MA. Interatomic potentials for describing impurity atoms of light elements in fcc metals. *Materials Physics and Mechanics.* 2019;42(4): 380-388.
22. Poletaev GM. Self-diffusion in liquid and solid alloys of the Ti-Al system: molecular-dynamics simulation. *Journal of Experimental and Theoretical Physics.* 2021;133(4): 455-460.
23. Poletaev GM, Starostenkov MD. Dynamic collective displacements of atoms in metals and their role in the vacancy mechanism of diffusion. *Physics of the Solid State.* 2009;51(4): 727-732.
24. Friedel J. *Dislocations*. Oxford: Pergamon press; 1964.
25. Hirth JP, Lothe J. *Theory of Dislocations.* 2nd ed. NY: Wiley; 1982.
26. Goldschmidt HJ. *Interstitial Alloys*. London: Butterworths; 1967.
27. Poletaev GM, Zorya IV, Rakitin RY, Glubokova LG. The binding energy of impurity atoms C, N, O with edge dislocations and the energy of their migration along dislocation core in Ni, Ag, Al. *Materials Physics and Mechanics.* 2020;44(3): 404-410.
28. Veiga RGA, Goldenstein H, Perez M, Becquart CS. Monte Carlo and molecular dynamics simulations of screw dislocation locking by Cottrell atmospheres in low carbon Fe-C alloys. *Scripta Materialia.* 2015;108: 19-22.

THE AUTHORS

Poletaev G.M.
e-mail: gmpoletaev@mail.ru
ORCID: 0000-0002-5252-2455

Rakitin R.Y.
e-mail: movehell@gmail.com
ORCID: 0000-0002-6341-2761